Electrochemical oxidation of 5-hydroxymethylfurfural on ternary metal-organic frameworks nanoarrays: enhancement from electronic structure modulation†

Xiao-Jue Bai,‡[a] Wen-Xiu He,‡[a] Xing-Yu Lu,[b] Yu Fu*[a] and Wei Qi*[b]

a. Department of Chemistry, College of Sciences, Northeastern University Shenyang 110819, China

E-mail: fuyu@mail.neu.edu.cn

b. Shenyang National Laboratory for Materials Science, Institute of Metal Research, Chinese Academy of Sciences, Shenyang, 110016, China.

E-mail: wqi@imr.ac.cn.

Experiment section

Materials

Cobalt chloride hexahydrate ($CoCl_2 \cdot 6H_2O$), nickel chloride hexahydrate ($NiCl_2 \cdot 6H_2O$), ferrous chloride tetrahydrate ($FeCl_2 \cdot 4H_2O$), 2-amino-terephthalic acid ($H_2BDC\text{-}NH_2$), 1,4-benzenedicarboxylate (H_2BDC), potassium hydroxide (KOH), and 5-hydroxymethylfurfural were purchased from Energy Chemical (Shanghai). N, N-Dimethylformamide (DMF) and ethanol (C_2H_5OH) were purchased from Sinopharm Chemical Reagent Co., Ltd. The water used in this work was deionized water. All chemicals used in this study were of analytical grade and used without further purification.

Preparation of MOFs/NF electrode

A certain amount of metal salt was dissolved in 32 ml DMF, 2 ml ethanol, and 2 ml H_2O. *($NiCl_2 \cdot 6H_2O$ (1.6 mmol) for Ni-MOFs/NF, $NiCl_2 \cdot 6H_2O$ (0.8 mmol) and $CoCl_2 \cdot 6H_2O$ (0.8 mmol) for CoNi-MOFs/NF, $NiCl_2 \cdot 6H_2O$ (0.8 mmol) and $FeCl_2 \cdot 4H_2O$ (0.8 mmol) for NiFe-MOFs/NF, $NiCl_2 \cdot 6H_2O$ (0.56 mmol), $CoCl_2 \cdot 6H2O$ (0.56 mmol), and $FeCl_2 \cdot 4H_2O$ (0.56 mmol) for CoNiFe-MOFs/NF)*

$H_2BDC\text{-}NH_2$ (1.6 mmol, organic-ligand for CoNiFe-MOFs) and H_2BDC (1.6 mmol, organic-ligand for Ni-MOFs, CoNi-MOFs, and NiFe-MOFs) was respectively dissolved in another 32 ml DMF, 2 ml ethanol, and 2 ml H_2O. The above solution was mixed under 10 min ultrasonication. Then the mixture solution was transferred into a 100 mL Teflon-lined autoclave with pre-cleaned Ni foams (NF) placed inside at an

inclined angle. This solvothermal reaction was performed at 150 °C for 12 h. After the autoclave was cool to room temperature, the product loaded on NF was collected at the bottom of the autoclave reactor and respectively washed with DMF and ethanol for three times, then dried in room temperature to obtain MOFs/NF electrode. For further characterization, MOFs were scraped from the MOFs/NF composites.

Characterization

Morphologies of samples were characterized by field-emission scanning electron microscopy (FESEM, Hitachi SU8010), transmission electron microscopy (TEM, JEOL JEM2100PLUS). The crystallographic information was analyzed by X-ray diffraction (XRD, PANalytical Empyrean) equipped with a Cu Kα radiation source (λ = 1.5406 Å). The organic groups in CoNiFe-MOFs were characterized by Fourier transform infrared spectroscopy (FT-IR, Bruker VERTEX 70). The composition of the materials was analyzed through quantitative X-ray photoelectron spectroscopy (XPS) which gave information about the surface electronic states of the elements (THERMO VG ESCALAB250). The products were analyzed by High Performance Liquid Chromatography (HPLC, Elite DG230-2) equipped with a UV-visible detector.

Electrochemical Tests

The electrochemical tests for OER and HMF oxidation were performed on a CHI 660E electrochemical workstation with standard three-electrode system, using MOFs/NF as working electrode, a Platinum sheet as counter electrode, and an Ag/AgCl as reference

electrode. Liner sweep voltammetry (LSV) curves of OER were tested at a scan rate of 5 $mV \cdot s^{-1}$ ranged from 1.0 V to 1.8 V (vs RHE) in an O_2-saturated 1.0 M KOH solution in undivided cell. LSV curves in of HMF oxidation were tested at a scan rate of 5 $mV \cdot s^{-1}$ in separated H-type electrochemical cell. Constant potential electrolysis test of HMF oxidation was operated at 1.40 V (vs RHE) in H-type electrochemical cell. The electrochemical double layer capacitance (C_{dl}) was obtained by cyclic voltammetry (CV) measurement at different scan rates of 20, 40, 60, 80, and 120 $mV \cdot s^{-1}$ in H-type electrochemical cell.

Products quantification

HPLC (Elite DG230-2), which detector is an ultraviolet-visible detector, was applied to analyze HMF oxidation products. Specifically, 10 μl of electrolyte was removed during constant potential electrolysis and diluted to 10 times with ultrapure water. 6 μl solution of diluted electrolyte was analyzed by HPLC. The specific parameters are set as follows. The wavelength of the UV detector is set to 265 nm, mobile phase A was methanol and phase B was ammonium formate aqueous solution, the ratio of A and B is 3:7, flow rate is 0.5 ml min^{-1}. Using waters organic acid column (SinoChrom ODS-BP 5μm, 4.6 mm x 200 mm, E2715082), each separation lasts for 8.5 minutes.

Conversion of HMF, FDCA yield and faradaic efficiency were calculated according to equations (1), (2) and (3), respectively.

$$\text{HMF conversion (\%)} = [n(\text{HMF consumed}) / n(\text{HMF initial})] \times 100 \quad (1)$$

$$\text{FDCA yield (\%)} = [n(\text{FDCA}) / n(\text{HMF initial})] \times 100 \quad (2)$$

Faradaic efficiency (%) = [n (FDCA formed) / (Charge / (6 x F))] x 100 (3)

Where F is the Faraday constant (96485 $C \cdot mol^{-1}$) and n is the mol of reactant calculated from the concentration measured by HPLC.

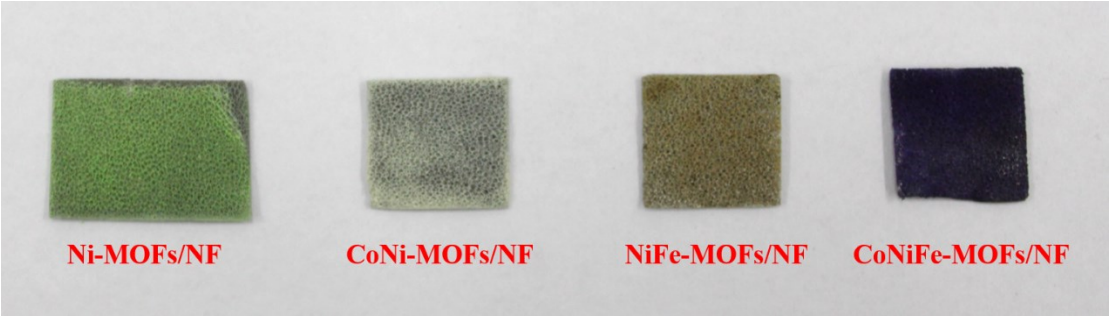

Fig. S1 Optical photographs of MOFs/NF. From left to right: Ni-MOFs/NF, CoNi-MOFs/NF, NiFe-MOFs/NF and CoNiFe-MOFs/NF.

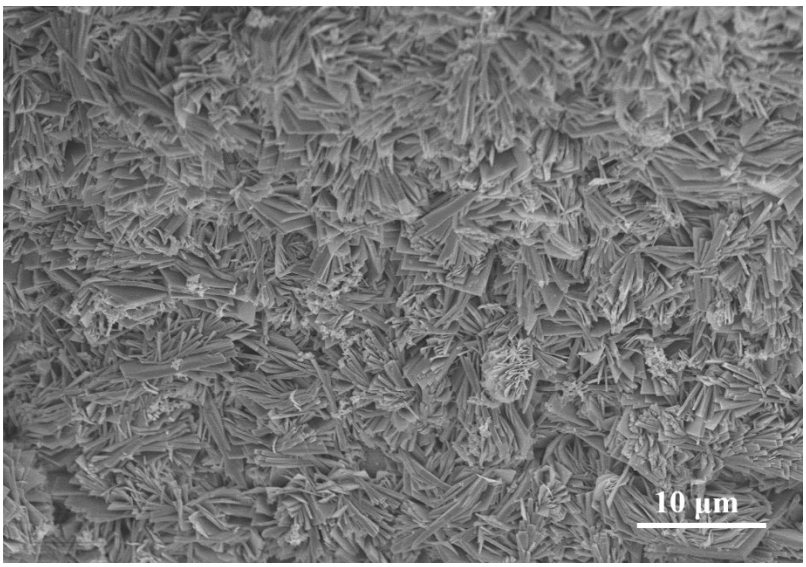

Fig. S2 SEM images of CoNiFe-MOFs/NF.

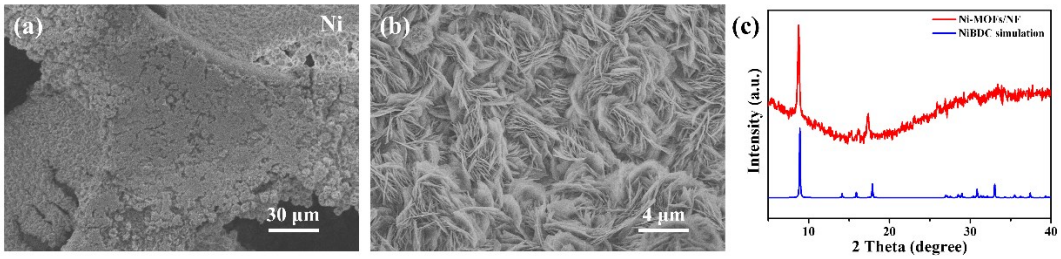

Fig. S3 (a) and (b) SEM images of Ni-MOFs/NF. (c) XRD patterns of Ni-MOFs/NF.

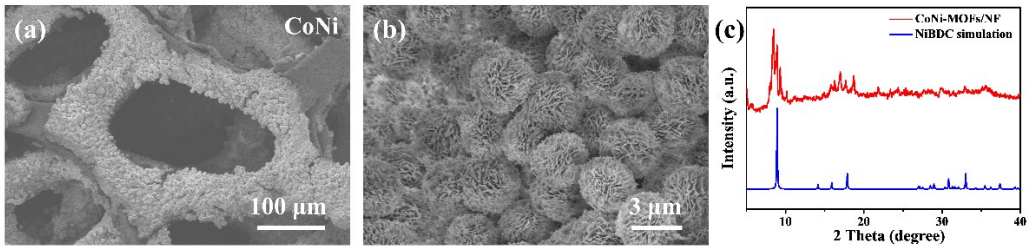

Fig. S4 (a) and (b) SEM images of CoNi-MOFs/NF. (c) XRD patterns of CoNi-MOFs/NF.

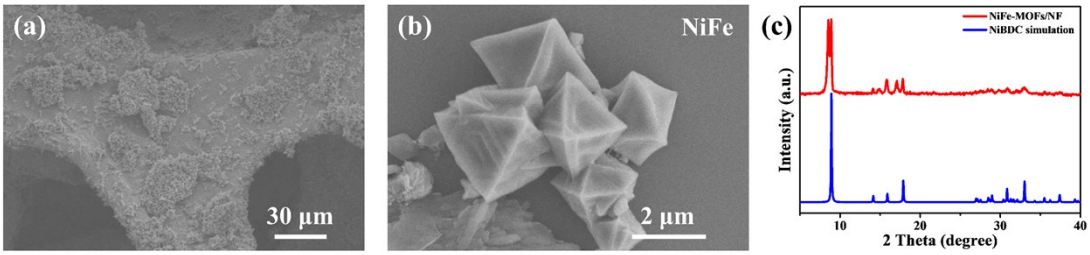

Fig. S5 (a) and (b) SEM images of NiFe-MOFs/NF. (c) XRD patterns of NiFe-MOFs/NF.

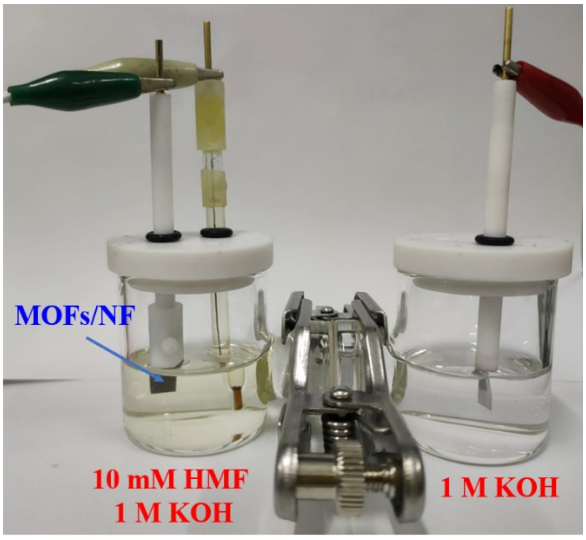

Fig. S6 Photograph of H-type electrolytic cell for electrochemical HMF oxidations.

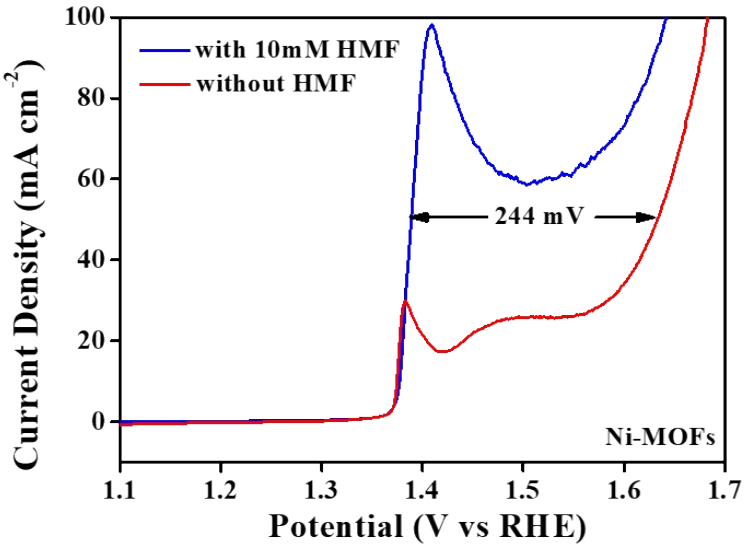

Fig. S7 LSV curves of Ni-MOFs/NF at the scan rate of 5 mV/s with and without 10 mM HMF.

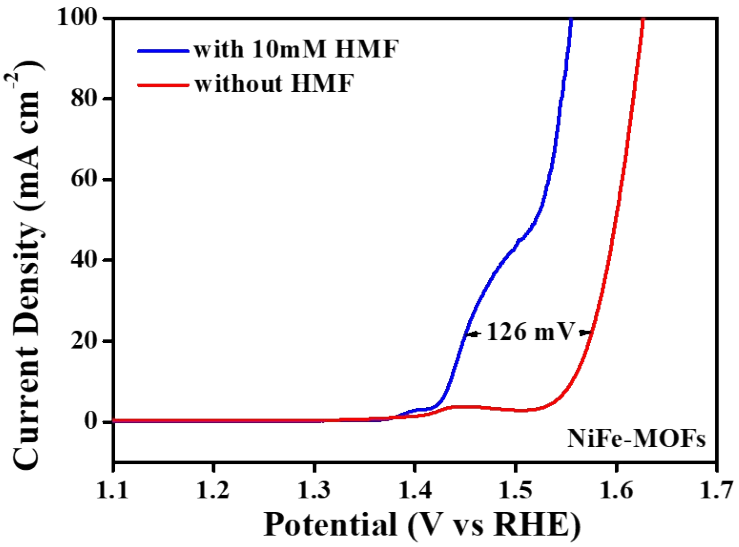

Fig. S8 LSV curves of NiFe-MOFs/NF at a scan rate of 5 mV/s with and without 10 mM HMF.

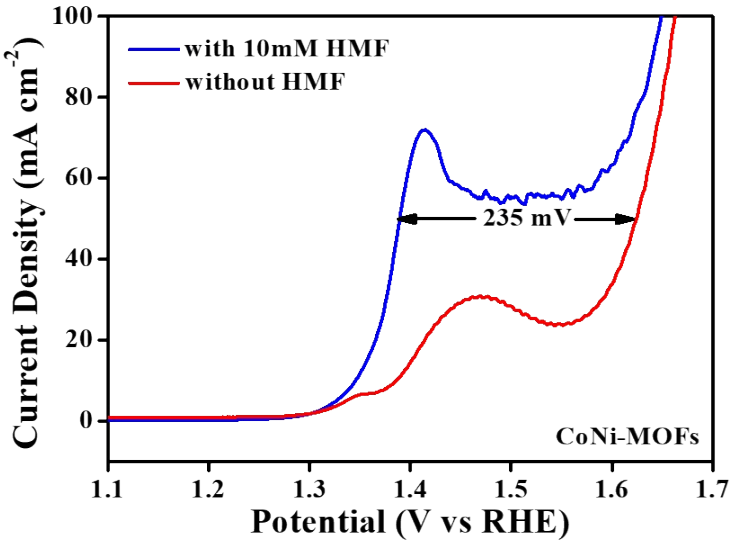

Fig. S9 LSV curves of CoNi-MOFs/NF at a scan rate of 5 mV/s with and without 10 mM HMF.

Table S1. Comparisons of the catalytic performance of different catalysts.

Electrocatalyst	**Potential (V) @ j ($mA \cdot cm^{-2}$)**	**Potential applied (V)**	**C_{HMF} (mM)**	**FDCA yield (%)**	**Faradaic efficiency (%)**	**Ref.**
CoNiFe-MOFs/NF	1.35@100	1.40	10	99.76	~100	This work
Ni_xB modified NF	1.45@100	1.45	10	98.5	~100	1
$NiCo_2O_4$	1.53@14.83	1.50	5	90.8	87.5	2
NiCoFe-LDHs	1.51@20	1.52	10	~85	~90	3
Ni_3N@C	1.38@50	1.45	10	98	99	4
$CuCo_2O_4$	1.37@150	1.45	10	93.7	94	5
CoO-$CoSe_2$	--	1.43	10	99	97.9	6
NiSe@NiO_x	1.36@240	1.423	10	99	99	7
TpBpy-Ni@FTO	--	1.55	0.5	58	--	8
NiOOH	--	1.47	5	96	96	9
nanocrystalline Cu foam	--	1.62	5	96.4	95.3	10

Reference:

1. S. Barwe, J. Weidner, S. Cychy, D. M. Morales, S. Dieckhofer, D. Hiltrop, J. Masa, M. Muhler, W. Schuhmann, *Angew. Chem. Int. Ed.* **2018**, *57*, 11460-11464.

2. M. J. Kang, H. Park, J. Jegal, S. Y. Hwang, Y. S. Kang, H. G. Cha, *Appl. Catal. B-Environ.* **2019**, *242*, 85-91.

3. M. Zhang, Y. Q. Liu, B. Y. Liu, Z. Chen, H. Xu, K. Yan, *ACS Catal.* **2020**, *10*, 5179-5189.

4. N. N. Zhang,Y. Q. Zou, L. Tao, W. Chen, L. Zhou, Z. J. Liu, B. Zhou, G. Huang, H. Z. Lin, S. Y. Wang, *Angew.Chem. Int. Ed.* **2019**, *58*,15895-15903.

5. Y. X. Lu, C. L. Dong, Y. C. Huang, Y. Q. Zou, Z. J. Liu, Y. B. Liu, Y. Y. Li, N. H. He, J. Q. Shi, S. Y. Wang, *Angew.Chem. Int. Ed.* **2020**, *59*,19215-19221.

6. X. Huang, J. L. Song, M. L. Hua, Z. B. Xie, S. S. Liu, T. B. Wu, G. Y. Yang, B. X. Han, *Green Chem.* **2020**, *22*, 843-849.

7. L. F. Gao, Z. B. Liu, J. L. Ma, L. J. Zhong, Z. Q. Song, J. Xu, S. Y. Gan, D. X. Han, L. Niu, *Appl. Catal. B-Environ.* **2020**, *261*,118235.

8. M. Cai, S. Ding, B. Gibbons, X. Z. Yang, M. C. Kessinger, A. J. Morris, *Chem. Commun.* **2020**, *56*,14361-14364.

9. B. J. Taitt, D. H. Nam, K. S. Choi, *ACS Catal.* **2019**, *9*, 660-670.

10. D. H. Nam, B. J. Taitt, K. S. Choi, *ACS Catal.* **2018**, *8*, 1197-1206.

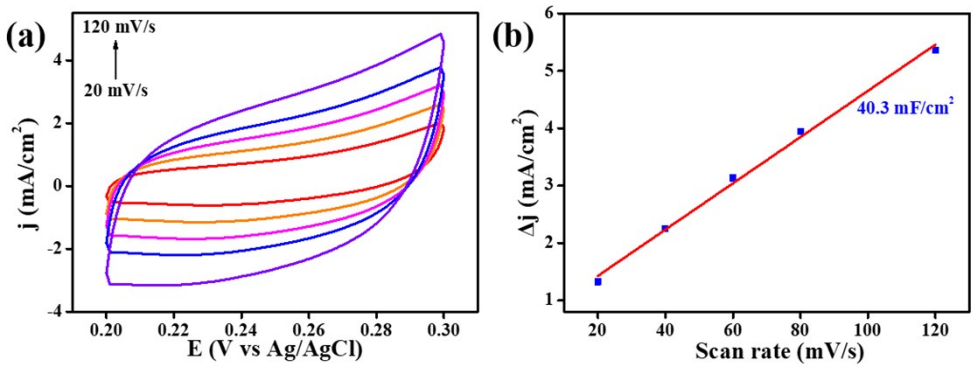

Fig. S10 (a) CV cycles of CoNiFe-MOFs/NF at di□erent scan rates from 20 mV/s to 120 mV/s, (b) the capacitive currents as a function of the scan rate (0.25 V).

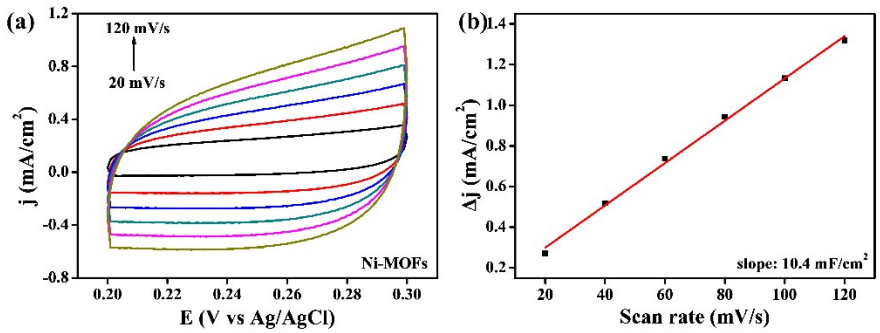

Fig. S11 (a) CV cycles of Ni-MOFs/NF at different scan rates from 20 mV/s to 120 mV/s, (b) the capacitive currents as a function of the scan rate (0.25 V).

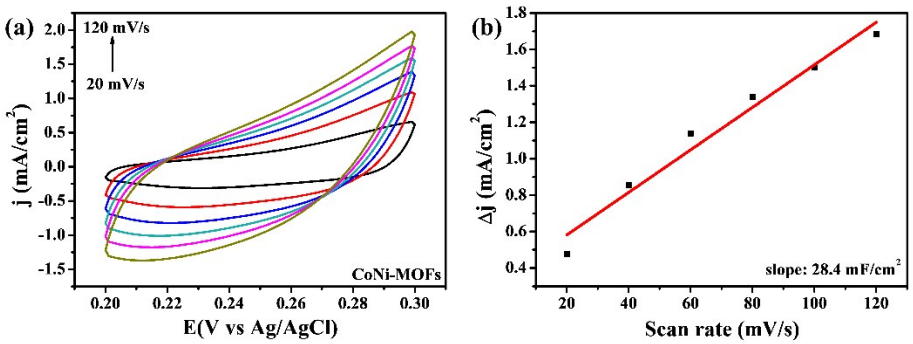

Fig. S12 (a) CV cycles of CoNi-MOFs/NF at different scan rates from 20 mV/s to 120 mV/s, (b) the capacitive currents as a function of the scan rate (0.25 V).

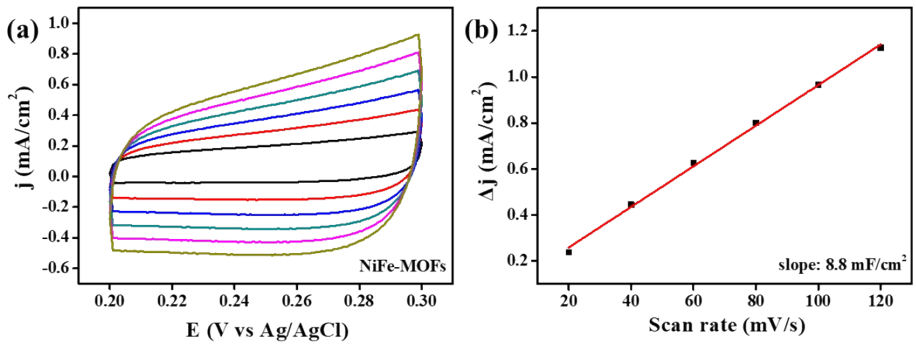

Fig. S13 (a) CV cycles of NiFe-MOFs/NF at different scan rates from 20 mV/s to 120 mV/s, (b) the capacitive currents as a function of the scan rate (0.25 V).

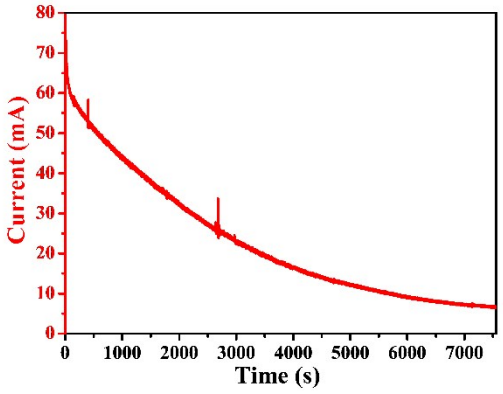

Fig. S14 Current-time curve during constant potential electrolysis using CoNiFe-MOFs/NF as the working electrode for the second cycle.

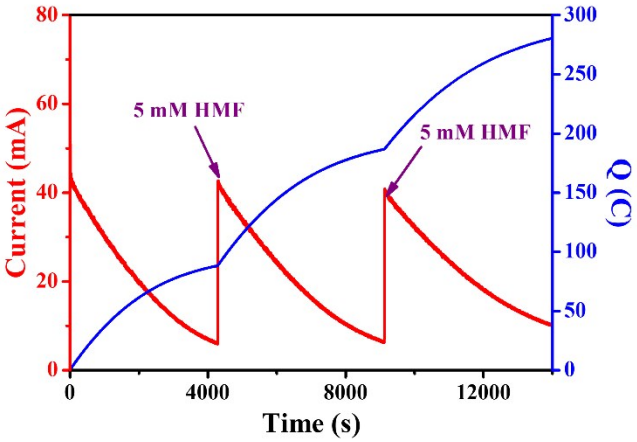

Fig. S15 Current and accumulated charge over the time with the addition of 5 mM HMF.

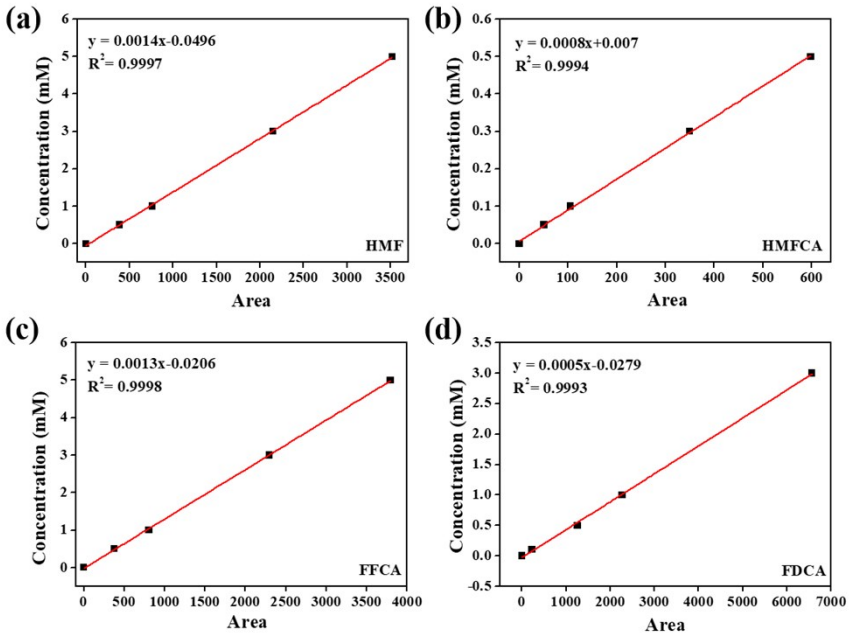

Fig. S16 The standard curve and corresponding equation of HMF, HMFCA, FFCA and FDCA obtaining by HPLC.

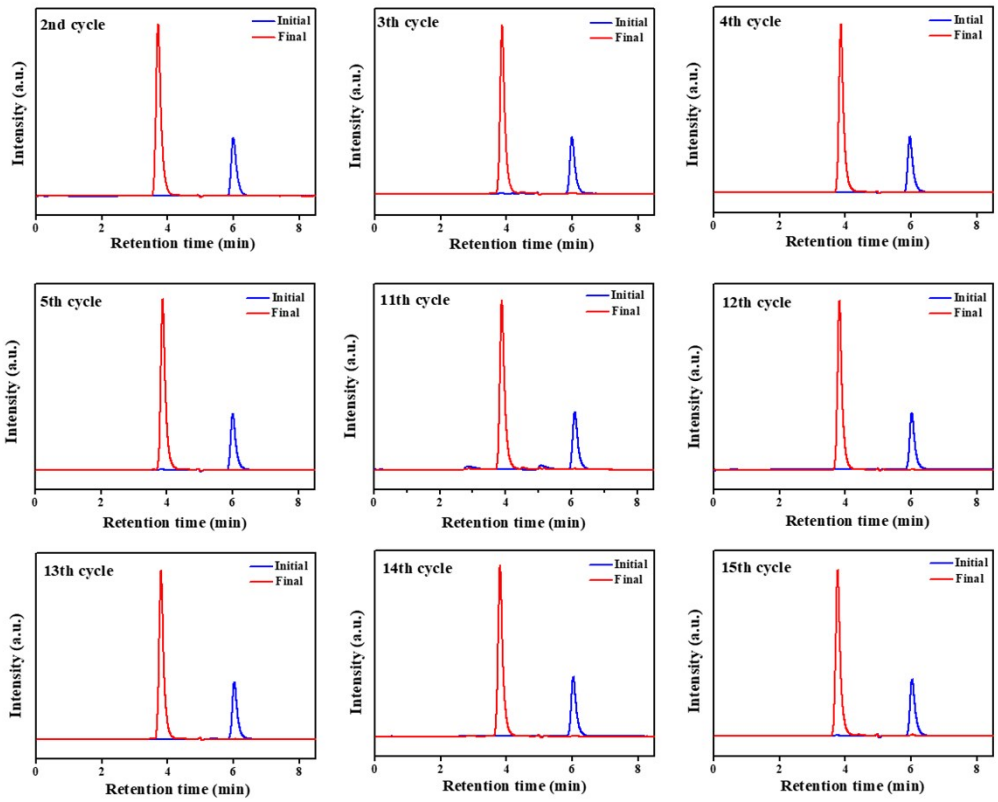

Fig. S17 The HPLC chromatograms for consecutive cycles for HMF oxidation.

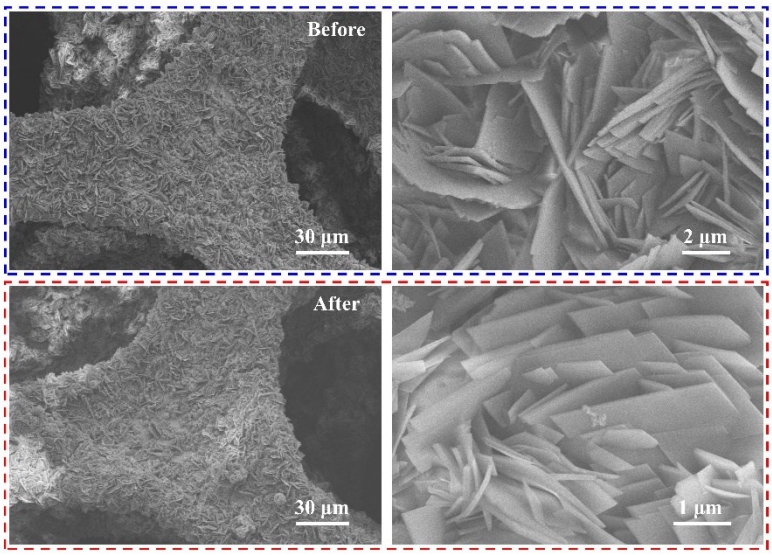

Fig. S18 SEM images of CoNiFe-MOFs/NF before and after ultrasonic treatment.